Green Chemistry

PAPER

View Article Online
View Journal | View Issue

Check for updates

Cite this: *Green Chem.*, 2026, **28**, 8938

Controlled release of chemically diverse small molecules from liquid-core capsules assembled under fully aqueous conditions

Rita C. Neves,† Bárbara S. Neves,† Bruno P. Morais, Raquel C. Gonçalves, João F. Mano and Mariana B. Oliveira *

The production of most molecule-release systems, including those used in the pharmaceutical industry, typically depends on traditional organic-solvent methods or energy-intensive thermal processes. The use of water as a solvent, processed under mild environmental conditions, can provide a cleaner, safer, and more environmentally friendly fabrication option. However, the inherently large mesh size of typical hydrogels has hindered the effectiveness of carrier systems processed under fully aqueous conditions for the controlled delivery of small molecules, which comprise more than 90% of currently approved drugs. Here, we report the development of stable liquid-core capsules, made of two polyelectrolytes derived from renewable sources, alginate and ε-poly-L-lysine-, with the ability to modulate both the entrance and release of small hydrophilic molecules with diverse charge properties. The low permeability features of the capsules prepared with water as the sole solvent were imparted by a post-processing step with the natural polyphenol tannic acid. The role of capsule size in the release profile of small molecules was addressed: treated capsules with diameters of *ca.* 3 mm, as well as their miniaturized counterparts with *ca.* 600 μm, supported the delayed release of small molecules. Their control counterparts, on their turn, led to burst release profiles typical of large mesh size polymeric systems. The developed platform offers a fully aqueous route to engineer controlled release systems, with potential impact in applications that may benefit from the tailored delivery of small molecules, including drug administration, precision agriculture, and miniaturized reactors.

Received 16th March 2026,
Accepted 5th May 2026

DOI: 10.1039/d6gc01588c

rsc.li/greenchem

Open Access Article. Published on 06 May 2026. Downloaded on 6/20/2026 10:08:09 AM.
This article is licensed under a Creative Commons Attribution 3.0 Unported Licence.

Green foundation

1. Our work advances green chemistry by developing an all-aqueous method for encapsulating and releasing small molecules, without using any organic solvents, energy-consuming protocols, or synthetic polymers.
2. We created a fully water-processed encapsulation method using algae-derived and microbial fermentation products, as well as tannic acid to form liquid-core capsules. The process fully eliminates the need for the use of organic solvents or high pressure and temperature. Additionally, the incorporation of a liquid water-based core in the devices enables reducing solvent waste.
3. Future work could optimize renewable component sourcing and minimize water use, the latter by developing localized in-air complexation strategies. Adapting the process to continuous manufacturing could also enhance its environmental and industrial impact.

Introduction

Small molecules (<1000 Da) comprise more than 90% of currently approved drugs,[1] as well as a major part of agricultural products including pesticides and fertilizers (*e.g.*, ref. 2). The localized and controlled release of molecules in the human body allows achieving optimized therapeutic efficacy and decreases risks of drug overdose.[3] In other fields, including agriculture, the localized delivery of molecules is considered a promising strategy to minimize unnecessary leaching to the environment, preventing the contamination of soil and water.[4] Space and time-controlled release of cargo is often achieved through incorporation into carrier materials. Mechanisms of molecular diffusion usually regulate molecular release kinetics, although strategies based on the controlled degradation of carriers have also been widely explored.[5,6]

The fabrication process of most molecule-release systems, including those used by the pharmaceutical industry, often relies on the use of classical organic solvent-based methods or

CICECO – Aveiro Institute of Materials, Department of Chemistry, University of Aveiro. Campus Universitário de Santiago, 3810-193 Aveiro, Portugal.
E-mail: mboliveira@ua.pt
† Equal author contribution.

This journal is © The Royal Society of Chemistry 2026

Open Access Article. Published on 06 May 2026. Downloaded on 6/20/2026 10:08:09 AM. This article is licensed under a Creative Commons Attribution 3.0 Unported Licence.

high-energy demanding thermal processes.[7] Using water as a working agent may be useful in circumventing the environmental burden and safety constraints associated with the use of volatile and toxic organic solvents.[1,8] Naturally occurring low-cost edible polymers and protein-based products, such as alginate and gelatin, are promising alternatives and soluble in water-based solvents. Although these polymers have been used in the pharmaceutical industry over the last decade, most applications rely on fast-release capsules for oral administration with fast dissolving properties (*e.g.*, ref. 9).

It is well reported that the processing of water-soluble materials often culminates in the generation of hydrogels or similar structures with pore sizes in the range of nanometers to micrometers.[10,11] Small molecules comprise sizes in the angstrom range, making their retention in those structures challenging, often presenting fast and burst-like release profiles through diffusion.[6] Approaches to control the release of small drugs, particularly those with hydrophilic character, have mostly relied on exploring their affinity with specific polymeric matrices,[12] for example, through electrostatic interactions and weak bonds established with the carrier matrix.[6,13,14]

Few approaches have focused on the universal control of permeability of hydrogel structures through the modulation of pore size. For example, some approaches relied on the design of bulk hydrogel-in-hydrogel setups for the creation of successive barriers for diffusion.[7,13] More recently, the addition of nanoparticles to continuous hydrogels[15] was explored with nanoparticles hypothesized to act in two ways: as physical fillers of hydrogel pores and as drug-binding agents. When interactions between small molecules and the carrier matrices significantly contribute to the retention/slow diffusion,[15] the use of continuous hydrogel architectures may promote drug retention in a radial size-dependent manner, making the initial distance of encapsulated molecules to the release medium a well-reported parameter for release kinetics.[16] Liquid-core capsules, surrounded by a thin wall, offer a liquid-filled space where molecules can be encapsulated with minimal interaction with materials. Minimizing contact between the loaded cargo and carrier materials could also allow for stability and long-term maintenance of structural features of sensitive molecules and facilitate the occurrence of reactions inside the capsules.

Herein, we propose that non-continuous liquid-core capsules with retentive membranes could work as close-to-scale independent versatile devices to achieve controlled release profiles of molecules with distinct chemistries. In the liquid core region of capsules, diffusion barriers are close to non-existent, as molecules move mostly freely. Therefore, control over the diffusion of molecules in liquid core/solid shell devices is expected to be solely controlled by membrane properties. The ability to produce liquid-core capsules with tailored permeability to diverse small molecules was explored by promoting the complexation of oppositely charged polyelectrolytes, treated with a natural polyphenol – tannic acid (TA). Small molecules with positive, negative, zwitterionic and neutral properties were used to validate the concept across a range of concentrations; the concept was then tested using capsules with diameters of *ca.* 600 μm and 3 mm. Given that a large number of pharmaceutical drugs are hydrophobic, which makes their encapsulation incompatible with fully aqueous conditions, a pilot study to understand the resistance of all-aqueous capsules to organic solvents was performed. Overall, we foresee that the proposed delivery system may find versatile applications such as in the development of drug delivery devices, and carriers for the precision delivery of pesticides and fertilizers, as well as the design of membrane-constrained miniaturized reactors compatible with water-based chemistries.

Experimental section

Materials

Epsilon-poly-L-lysine (EPL, Epolyly®, 4700 Da) from fermentation of *Streptomyces albulus* PD-1 was purchased from Handary S.A. (Brussels, Belgium). Alginic acid sodium salt (ALG, 120 000–190 000 Da, ref 71238) from brown algae, phosphate buffered saline (PBS) tablets, tannic acid (TA, 1701 Da) and hydrochloric acid (HCl) were acquired from Sigma-Aldrich (St. Louis, USA). Sodium hydroxide (NaOH) was purchased from Nouryon (Amsterdam, the Netherlands), acetic acid glacial 99–100% from Chem-Lab (Zedelgem, Belgium) and sodium acetate trihydrate AGR from Labkem (Barcelona, Spain). The ethanol solutions of 96% and 100% were obtained from Aga (Lisbon, Portugal) and Carlo Erba (Val-de-Reuil, France), respectively. Methylene Blue (MB, 320 Da) was purchased from Biosynth (Bratislava, Slovakia) while Allura Red AC (AR, 496 Da) was purchased from TCI Chemicals (Tokyo, Japan). Fast Green FCF (FG, 809 Da) was acquired from Sigma-Aldrich (St. Louis, USA). mPEG-FITC (linear monofunctional polyethylene glycol reagent conjugated with a fluorescein dye – FITC) (739.4 Da) was purchased from Biopharma PEG Scientific Inc. (Watertown, USA).

Methods

Production of macrocapsules and impermeability tests. EPL and ALG solutions were prepared following the previously reported concentrations of 0.75 wt% and 2 wt%, respectively,[13] by dissolving these in PBS, under stirring. The pH value of the EPL solution was then adjusted to 5, using HCl and NaOH solutions (1 mM) and a pH meter (Consort).

Using a syringe pump (Harvard Apparatus), with a flow rate of 1 mL min^{-1}, capsules were fabricated by dispensing a solution of ALG (phase I or droplet phase), using a 1 mL plastic syringe with a 21-gauge needle at a working distance of 15 cm from a 50 mL bath solution of EPL (phase II or bath phase). The phase II EPL solution was continuously stirred in a 100 mL beaker with a multipoint magnetic stirrer at 250 rpm during dispersion of the phase I ALG solution. After 5 minutes of complexation, one washing step was dynamically performed for 10 minutes, at 250 rpm, with a large volume of PBS. Capsules were post-treated with a solution of TA 0.4% (w/v), at

Open Access Article. Published on 06 May 2026. Downloaded on 6/20/2026 10:08:09 AM.
This article is licensed under a Creative Commons Attribution 3.0 Unported Licence.

pH 7, for 2 minutes. The resulting capsules were exposed to dye solutions (MB; AR; FG) for 60 minutes to assess membrane permeability to each dye.

Scanning electron microscopy (SEM). Scanning Electron Microscopy (SEM) analysis was performed to microscopically analyse the influence of the addition of TA to the capsules. Capsules without TA treatment (control) and with TA treatment were dehydrated by immersing them for 15 minutes in ethanol solutions following a concentration gradient of 30% (v/v), 50% (v/v), 70% (v/v), 80% (v/v), 90% (v/v), 96% (v/v) and 100% (v/v). To visualize the lumen, transversal cross-sections were made using a scalpel blade prior to dehydration. Samples were then coated with a gold/palladium film by sputtering for 3 minutes, to make them conductive and to allow better resolution of the images. Afterwards, capsules were imaged through SEM using an Ultra-high Resolution Analytical Scanning Electron Microscope HR-FESEM Hitachi SU-70 (Hitachi, Tokyo, Japan), with a voltage of 15.0 kV.

Encapsulation and release of low molecular weight molecules. Due to intrinsic properties and specific interactions of each dye with the capsule membrane and TA treatment, loading of low molecular weight molecules was performed using two different approaches (Fig. 2). Analysis and development of both procedures are thoroughly discussed in the Results section. Release studies were performed in PBS (pH 7.4) and acetate buffer (pH 4), ensuring that sink conditions were maintained. For initial studies, and also for testing the capsule resistance to organic solvents, the molar concentration (0.3 mM) was maintained for MB, AR and FG (0.10 to 0.20 mg mL^{-1} range). For mPEG-FITC, a concentration of 0.20 mg mL^{-1} was used. For studies with molecules at higher concentrations, AR was tested up to concentrations of 15 mg mL^{-1}, and 20 mg mL^{-1} for mPEG-FITC. All measurements were performed in triplicate, and the incubation conditions were 37 °C and 50 rpm. At each timepoint, 200 μL of the medium was collected and 200 μL of PBS buffer was added to each flask. Absorbance was read with a 96-well plate reader for each sample at the maximum wavelength for each dye (664 nm for MB; 504 nm for AR; and 625 nm for FG), and fluorescence at 495 excitation/519 nm emission for mPEG-FITC, for each collected sample, with a clear bottom black side plate, and data were presented as the cumulative released mass over time. For absorbance/fluorescence detection, 100 μL of the collect medium was recorded using a microplate reader (Synergy HTX), and the values were then analysed using Gen5 2.09 software.

Production of miniaturized capsules. Micrometric-sized capsules, ranging from 500 to 650 mm, were fabricated using an electrohydrodynamic atomization equipment (SKE Research Equipment, E-FIBER EF100, Electrospray). Phase II was used as a collector bath, containing 20 mL of EPL solution in a 50 mL beaker, and complexation occurred for 2 minutes. The operating parameters were a flow rate of 500 mL h^{-1}, a 22G needle, a tip-to-collector distance of 5 cm, and an applied voltage of 10 kV. After complexation, three washing steps were performed using PBS solution for 5 minutes, at 300 rpm, using a final volume of 40 mL in the beaker. 0.3 mM (0.10 mg mL^{-1}) mPEG-FITC was loaded for 3 hours, and the previously described TA treatment was performed afterwards.

Mechanical analysis. The mechanical behaviour of millimetric-sized capsules was assessed by compression testing using an Instron Uniaxial Testing Machine (INSTRON®, USA) equipped with a 50 N load cell. Values were determined using the Bluehill Universal software, version 4.29. Compression test data were collected for all replicates; the maximum compression strain and the toughness of the material were determined and presented graphically as mean ± standard deviation (SD) for 10 replicates. The as-prepared TA-treated capsules were subjected to a pre-load of 0.5 mm min^{-1} before each test, and samples were compressed until rupture at a deformation rate of 1 mm min^{-1}.

Fitting of release profiles to kinetic models. The release profiles obtained from the polymeric capsules were analysed by fitting the experimental data to several mathematical kinetic models, in order to characterise the mechanisms governing molecular transport across the membrane, using the MATLAB™ (MathWorks, USA) software. The models evaluated included zero-order, first-order, Higuchi, Korsmeyer–Peppas and Weibull models.

A custom script was developed to perform non-linear regression and estimate the kinetic parameters for each model. Model performance was assessed using statistical indicators including the coefficient of determination (R^2), sum of squared errors (SSE), root mean square error (RMSE) and Akaike information criterion (AIC). These parameters were used to compare the goodness of fit and identify the most appropriate model describing the release behaviour under the different experimental conditions.

Statistical analysis. Data are represented as mean ± standard deviation (SD) for 3 replicates. Statistical significance was analysed using One-Way ANOVA followed by Tukey's multiple comparisons test, using GraphPad Prism software 10.2.0 (GraphPad, Inc.); significance * was defined as $p < 0.05$; ** as $p < 0.01$; *** as $p < 0.001$; and **** as $p < 0.0001$.

Results and discussion

Fabrication and characterization of low permeability capsules

Capsules with liquid cores were prepared through the promotion of the complexation between alginate (ALG; reported $pK_a \approx 4.3–4.5$) and epsilon-poly-L-lysine (EPL; reported $pK_a \approx 8.8–9.7$).[17] Droplets of a solution of ALG (here named phase I) at pH 7 were dropped in a bath of EPL (phase II) at pH 5. Polyelectrolyte complexation was performed using polymer concentrations of 0.75 wt% EPL and 2 wt% ALG, in the absence of any phase-separating system, *i.e.* using phosphate buffered saline (PBS) as the only solvent of both polyelectrolytes to generate liquid core capsules (Fig. 1A and Fig. S1A from the SI). A working complexation time of 5 minutes was defined due to its compatibility with the high-yield production of robust capsules with diameters in the range of 2.8 to

 This journal is © The Royal Society of Chemistry 2026

Open Access Article. Published on 06 May 2026. Downloaded on 6/20/2026 10:08:09 AM.
This article is licensed under a Creative Commons Attribution 3.0 Unported Licence.

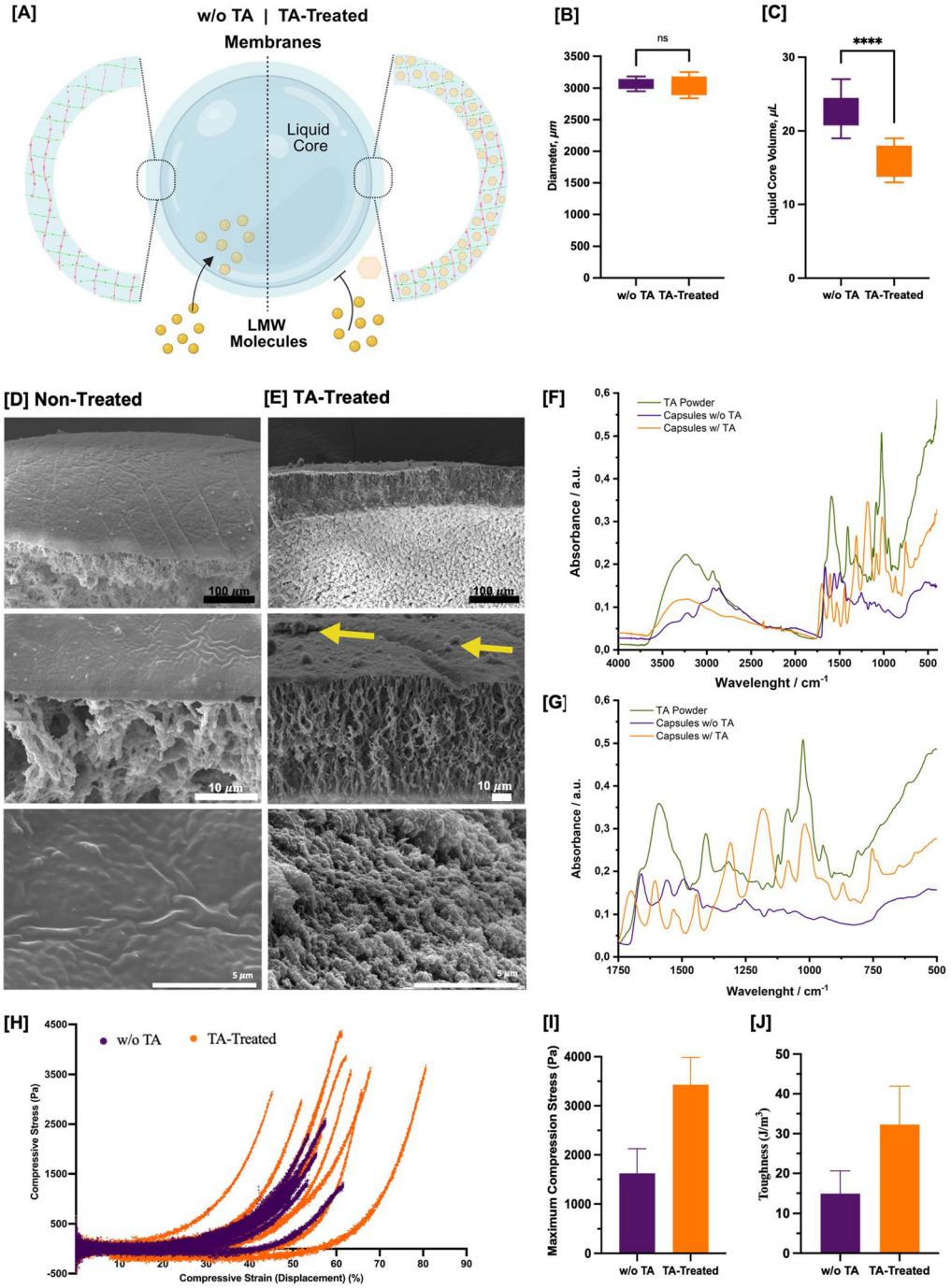

Fig. 1 Schematic representation of all processing steps of the system to enhance membrane properties. [A] Schematic representation of the capsules' membranes in the absence and presence of TA. [B] Morphological comparison between macrocapsules in the absence and presence of post-treatment under optimised conditions, highlighting changes in the diameter (n = 8) and [C] liquid core volume (n = 10). [D] SEM cross-section images of the control and TA-treated capsules. The surface of the control capsules was smooth, [E] while the surface of the TA-treated capsules had irregularities (highlighted with a yellow arrow), caused by an accumulation of TA in the outer region of the capsules. [F] FTIR-ATR spectra (4000–500 cm^{-1}) of polyelectrolyte liquid-core capsules and tannic acid powder. Capsules were freeze-dried prior to analysis. [G] Expanded fingerprint region (1750–500 cm^{-1}). In all spectra, brown lines denote tannic acid powder; purple lines indicate control capsules; and solid orange lines represent TA-treated capsules. [H] Representative stress–strain curves of 2% alginate/0.75% ε-poly-lysine capsules subjected to unidirectional compressive stress assays. Rheological data were obtained from twenty different capsules, with half of them analysed after TA-treatment at a concentration of 0.4% (w/v). In the graph, the purple curves correspond to control capsules, while the orange curves represent TA-treated capsules. [I] Maximum compressive stress of 2% alginate/0.75% ε-poly-lysine capsules obtained from unidirectional compressive stress assays. Purple bars represent control capsules (w/o TA), while orange bars correspond to TA-treated capsules (0.4% w/v). Error bars indicate standard deviation (n = 10). [J] Toughness of 2% alginate/0.75% ε-poly-lysine capsules obtained from unidirectional compressive stress assays. Purple bars represent control capsules (w/o TA), while orange bars correspond to TA-treated capsules (0.4% w/v). Error bars indicate standard deviation (n = 10).

Open Access Article. Published on 06 May 2026. Downloaded on 6/20/2026 10:08:09 AM.
This article is licensed under a Creative Commons Attribution 3.0 Unported Licence.

3.2 mm (Fig. 1B). Capsule size showed similarity to the initial sizes of the dispensed droplets. Processing parameters were selected following a previous report showing that core–shell tubes processed by pump-led extrusion enabled the high retention of 10 kDa FITC-labelled dextran when prepared in the absence of supporting aqueous two-phase systems.[13] Additionally, acidic pH values of the bath phase were previously shown to promote the formation of stable interface-complexed structures.[13] Therefore, a pH value of 5 for phase II was selected to further decrease the permeability of the prepared capsules (Fig. S1B–D, SI).

Additional optimization steps were performed to characterize the permeability of capsules prepared simply through the complexation of polyelectrolytes, and no further treatment (Fig. 2). An optimization pilot study was performed with capsules prepared under different conditions, including different times of complexation ranging from 2 to 15 minutes (Fig. S1E, SI). The ability of the prepared capsules to hamper the entrance of small molecules was then evaluated using a positively charged molecule – Methylene Blue (MB; 320 Da)-, and the negatively charged Allura Red (AR; 496 Da) (Fig. S1F, SI). None of the tested formulations presented significant retention or slowing down of the permeance of dyes to the inner liquid core of the capsules. The addition of a post-treatment with TA was hypothesized to decrease the molecular weight cut-off (MWCO) of the developed capsules. As a polyphenol, TA exhibits several hydroxyl groups that promote both intramolecular and intermolecular interactions by promoting the crosslinking between polyelectrolyte chains/complexes, and possibly through the ability of TA–TA nano- to micrometric constructs to block the pores of the formed polyelectrolyte membranes.[18–20] TA is labelled as GRAS by the Food and Drug Administration (FDA) and is used within limited concentrations in food and pharmaceutical industries and research, namely, to crosslink capsules and micelles.[15,18] All constituent materials of the system are widely available and can be obtained from natural sources such as algae for alginate, and vegetal sources for tannic acid;[21,22] for the case of EPL, its production through microbial fermentation has gone through scale-up procedures,[23] supporting its potential for large-scale implementation. TA was selected for its polyphenolic structure enabling multivalent interactions, aqueous compatibility, and alignment with green chemistry principles, while the model compounds (MB, AR) were chosen to span a range of charge characteristics within the sub-kDa regime.

The effect of the post-treatment of capsules with different concentrations of TA, at varying pH values and treatment times, was evaluated. Overall, the effectiveness of the TA coating in preventing the entrance of MB and AR into the liquid core of the capsules increased with higher TA concentrations and treatment times (Fig. S1D and E, SI). Lower TA concentrations required higher treatment times to be effective at preventing molecular crossing of the polymeric membranes. Based on these initial observations, a treatment consisting of the immersion of pre-made polyelectrolyte capsules in a solution of 0.4% TA at pH 7, for 2 minutes, was selected for further studies. Of note, the optimized treatment with TA did not significantly affect the measured outer diameter of the capsules; however, it led to a significant decrease in their average inner liquid volume, from 22 μL to 16 μL (Fig. 1B and C).

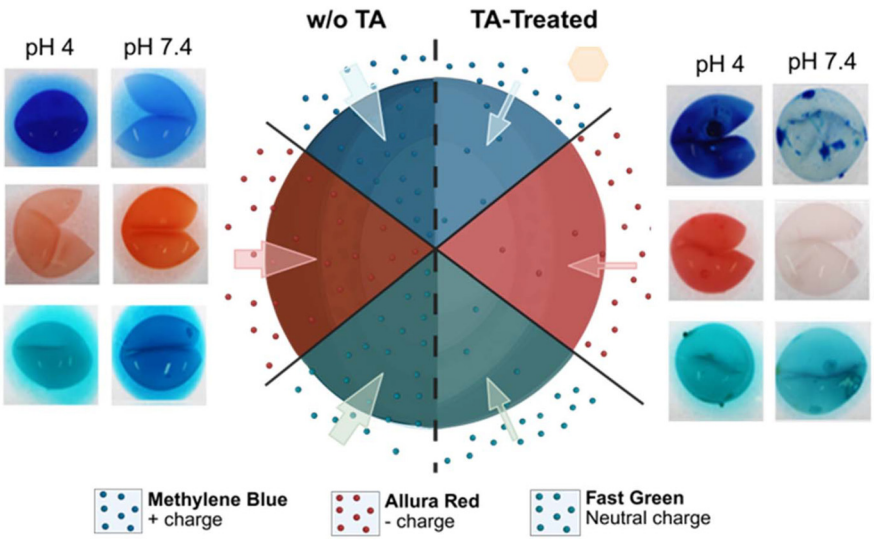

Fig. 2 Schematic representation of dye permeation across capsule membranes in the absence (w/o TA) and presence (w/TA) of tannic acid (TA). Visual representations of permeability and dye-membrane interactions are shown, after 1 hour of incubation, in solutions containing dyes with distinct molecular charges: Methylene Blue (MB, positively charged, 320 Da); Allura Red (AR, negatively charged, 496 Da) and Fast Green (FG, zwitterionic, neutral charge, 809 Da). Despite visual differences in dye distribution, permeation into the capsule core was observed under all conditions; however, the application of TA led to the formation of intermolecular interactions within the membrane, contributing to a more controlled diffusion of dyes, as indicated by the thinner inward arrows, suggesting an improvement in membrane selectivity in encapsulation strategies.

This journal is © The Royal Society of Chemistry 2026

Open Access Article. Published on 06 May 2026. Downloaded on 6/20/2026 10:08:09 AM. This article is licensed under a Creative Commons Attribution 3.0 Unported Licence.

Capsules were analysed by scanning electron microscopy (SEM) to address morphological alterations caused by the TA treatment (Fig. 1D and E). Control (non-treated) capsules were formed by a first layer of immediately reacted polyelectrolytes, followed by a tortuous and more dispersed inner region, similarly to the morphology of capsules and tubes previously assembled at the interfaces of aqueous two-phase systems (ATPSs).[13,17] Treated capsules showed an accumulation of TA in the outer less porous membrane, with some apparent aggregates (Fig. 1E), which may correspond to the formation of a non-uniform coating and larger TA–TA microstructures.[12,24] Those structures could not be found in their non-treated counterparts (Fig. 1D). No clear morphological indication of the presence of TA aggregates was observed by SEM in the inner and less dense regions of the capsules (Fig. 1E). Nonetheless, the presence of TA in the entire structure of the membranes was corroborated by the immersion of capsules in a 10 M NaOH solution. Unlike their control counterparts, TA-treated capsules immediately turned brownish throughout their entire structure, including the inner membrane (Fig. S2, SI). The observed change of colour is justified by the formation of quinones due to the oxidation of the TA catechol groups at high pH values.[8] Our results suggest that TA accumulates in the outer and more continuous membrane of the capsules, forming nanometric aggregates visible by SEM, while possibly smaller aggregate forms of TA–TA complexes and single TA molecules are present in the less dense inner part of the membranes. While surface-associated TA aggregates are observed, they cannot be exclusively identified as the sole factor driving the reduced permeability through pore clogging. In fact, TA-mediated supramolecular crosslinking within the polyelectrolyte network may contribute to a decrease in the effective mesh size of the system.

To further elucidate the molecular basis of the observed morphological alterations, vibrational spectroscopy was employed to probe the interactions between TA and the ALG/EPL membrane. Fourier Transform Infrared Spectroscopy with Attenuated Total Reflectance (FTIR-ATR) was employed to identify functional groups present in the system. The spectrum of TA powder displayed a broad absorption band in the 3500–3200 cm^{-1} region, characteristic of O–H stretching vibrations from phenolic hydroxyl groups. Additional strong bands were observed between 1700 and 1600 cm^{-1}, attributed to the C=O stretching of ester linkages and aromatic C=C vibrations, together with intense features in the 1200–1000 cm^{-1} region attributed to the C–O stretching of phenolic and ester moieties. Control capsules displayed the typical vibrational features of the Alg/EPL polyelectrolyte network (Fig. 1F). A broad band centred around 3400–3200 cm^{-1} was assigned to overlapping O–H stretching vibrations, while the asymmetric and symmetric stretching modes of alginate carboxylate groups appeared at approximately 1610–1590 cm^{-1} and 1420–1400 cm^{-1}, respectively (Fig. 1G). Additional contributions in this region arise from amide vibrations associated with EPL. Following TA treatment, several subtle but consistent spectral modifications were observed. The O–H stretching region exhibited noticeable band broadening, indicating enhanced hydrogen-bonding interactions within the membrane environment. In addition, a moderate increase in peak intensity within the 1600–1500 cm^{-1} region was detected, probably related to the overlapping contributions from aromatic vibrations of TA and the carboxylate/amide bands of the Alg/EPL network. Changes were also observed in the 1200–1000 cm^{-1} region, where slightly increased band definition and intensity suggest the incorporation of phenolic structures associated with TA (Fig. 1G). Importantly, no additional absorption bands characteristic of covalent bond formation were detected. In particular, no new bands appeared in the 1685–1660 cm^{-1} region, which could be attributed to quinone C=O stretching, nor were distinct bands observed in the 1650–1620 cm^{-1} region attributable to imine (C=N) formation. These observations indicate that TA does not induce detectable covalent crosslinking within the membrane, and instead interacts primarily through non-covalent interactions, including hydrogen-bonding and electrostatic associations between phenolic groups and the functional groups of the Alg/EPL network.[25] A small blue shift of specific bands was also observed after TA treatment (Fig. 1F). In the present system, this behaviour suggests a rearrangement and local tightening of the polyelectrolyte network upon TA adsorption, likely resulting from the formation of additional hydrogen-bonding interactions between TA phenolic groups and the membrane polymers.

Raman spectroscopy was also employed to further characterize the different capsules. The technique probes molecular vibrations through inelastic photon scattering.[26,27] In this study, only the Stokes region of the Raman spectra was analysed to evaluate possible structural changes within the ALG/EPL membrane following TA coating. The Raman spectrum of TA powder (Fig. S3A, SI) exhibited strong aromatic C=C stretching bands around 1600 cm^{-1}, together with phenolic-associated modes in the 1350–1300 cm^{-1} region and additional aromatic ring-breathing vibrations below 1000 cm^{-1}, which are characteristics of polyphenolic structures. In comparison, both control and TA-treated capsules displayed highly similar spectral profiles (Fig. S3B and C, SI), indicating the preservation of the structural framework of the Alg/EPL polyelectrolyte membrane. Due to the substantially higher concentration of pure TA powder relative to the thin capsule membrane, the raw spectra of TA powder exhibited markedly higher signal intensity. After spectral normalization, a slight increase in peak intensity around 1600 cm^{-1} was observed for TA-treated capsules (Fig. S3C, SI), consistent with the presence of aromatic functionalities originating from tannic acid at the capsule interface. Minor variations were also detected between 1400 and 1200 cm^{-1}, a region associated with phenolic ring modes. Notably, no new Raman bands were detected in the 1680–1650 cm^{-1} region, where quinone C=O vibrations would typically appear, nor were additional bands observed in the 1650–1620 cm^{-1} region that could be attributed to imine (C=N) formation.

Open Access Article. Published on 06 May 2026. Downloaded on 6/20/2026 10:08:09 AM. This article is licensed under a Creative Commons Attribution 3.0 Unported Licence.

Taken together, Raman and FTIR-ATR analyses consistently indicate that TA interacts with the ALG/EPL membrane predominantly through non-covalent interactions, while preserving the fundamental chemical structure of the polyelectrolyte complex, which is supported by the absence of newly formed vibrational bands. This spectroscopic interpretation is consistent with mechanical analysis, which further corroborated the presence of TA within the capsule membrane and its effect on membrane crosslinking. TA-treated capsules exhibited higher elastic modulus and increased resistance to rupture (Fig. 1H and I). Such behavior suggests that TA promotes additional intermolecular interactions within the membrane, leading to a denser and mechanically reinforced polymeric network, thus increasing its toughness (Fig. 1J), likely accompanied by partial dehydration of the membrane structure (Fig. 1C). These mechanical properties may be particularly interesting when exposed to mechanical demanding settings, such as in the gastrointestinal tract, or implanted in tissues subjected to compression forces.

The stability of the TA coating on the capsule membranes was also assessed by monitoring TA release over a 24-hour period. TA was detected in the surrounding medium shortly after immersion in both PBS and acetate buffer, indicating an initial release from the membrane surface. Higher TA concentrations were measured in PBS, where a gradual increase in TA levels was observed during the first 6 hours of incubation (Fig. S4, SI). These results suggest that while a fraction of loosely associated TA is released upon immersion, a significant portion of the coating remains associated with the membrane structure.

A comparative perspective on the "green" features of the developed technology

The platform for small molecule delivery described here adapts to the "benign by design" approach, correlated with the 12 key principles of green chemistry.[28] The technology aligns with 7 of those principles. Unlike traditional pharmaceutical encapsulation methods that frequently rely on organic solvents and energy-intensive processing steps,[7] the described encapsulation devices are fabricated entirely with water as a solvent, eliminating volatile organic compounds and minimizing waste that requires extensive treatment, therefore aligning with (1) prevention, (2) safer solvents and auxiliaries, and (3) less hazardous chemical synthesis principles. Additionally, besides the use of water as a sole solvent, alginate (ALG) and poly-L-lysine (EPL) are approved for food additives, and tannic acid is considered GRAS.[15,18] Capsules are composed mainly of two polyelectrolytes obtained from renewable sources – brown algae for ALG and microbial fermentation for EPL, aligning with the (4) use of renewable feedstocks. The entire workflow from solution preparation to the final stages of release studies can be performed without any special safety measures, besides the use of standard laboratory individual safety equipment (*i.e.*, lab coat, safety glasses, and nitrile gloves). Extraction systems for the generated gases are not necessary. The safe handling of the initial materials and fabricated capsules aligns with the principle[6] of inherently safer chemistry for accident prevention. Both capsule formation and tannic acid treatment occur under mild, ambient conditions, reducing energy consumption and improving safety relative to solvent-based or thermally driven encapsulation routes – (6) design for energy efficiency. Additionally, the developed capsules retain a high amount of water as part of their functional structure, and all alginate reacts to form capsule shells, leading to a high efficiency of the use of initial materials – (7) reduce derivatives. Together, these features demonstrate that the platform offers an environmentally conscious route for small-molecule encapsulation, highly consistent with modern green-chemistry principles.

A comparison between typical encapsulation methods used by the pharmaceutical industry (Table 1)[6] and with the most well-established counterpart for all-aqueous liquid-core capsule manufacturing – layer-by-layer (LbL) deposition followed by the dissolution of a solid template (ref. 7 and 29; Table 2) – is provided. An estimation of the generation of waste materials is provided through the calculation of an *E*-factor[30] to compare the herein proposed technology with all-aqueous LbL methodologies (Table S1, SI).

Table 1 Comparison with classic encapsulation methods[6,7]

Criterion	Classic encapsulation methods (organic solvent-based, reactive crosslinkers, synthetic polymers)	Present work (liquid-core capsules with TA-densified shell)	Green advance
Processing medium	Frequently requires organic solvents or activation buffers	Fully aqueous	100% elimination of organic solvents
Crosslinker strategy	Covalent crosslinkers (*e.g.*, EDC/NHS, glutaraldehyde), derivatization steps	Supramolecular interactions with tannic acid	Avoids hazardous reagents; low/no chemical derivatization
Polymers/solvents	Synthetic, often non-biodegradable polymers; organic solvents	Renewable, biodegradable polymers; water as a solvent	Residues with low requirements for treatment before discarding
Water consumption	Large amount	Low (one washing step); incorporation of water as a capsule component	Major reduction in water usage
Energy demand	Heating, evaporative drying, high-energy emulsions	Environmental temperature processing	Substantial reduction in energy consumption
Safety profile	Toxic solvents, reactive reagents, strict containment	Non-toxic, food-grade materials	Inherently safer processing
Waste treatment	Solvent recovery or specialized disposal required	Standard aqueous waste	Simplified downstream handling

 This journal is © The Royal Society of Chemistry 2026

Open Access Article. Published on 06 May 2026. Downloaded on 6/20/2026 10:08:09 AM. This article is licensed under a Creative Commons Attribution 3.0 Unported Licence.

Table 2 Comparison with other water-based systems: conventional continuous hydrogels, and all-aqueous sacrificial template-based layer-by-layer (LbL) assemblies[6,7]

Criterion	Conventional hydrogels (*e.g.*, alginate, gelatin, PEG)	LbL capsules	Present work (liquid-core capsules with TA-densified shell)
Release mechanism	Diffusion through large aqueous pores, burst release	Diffusion across multilayers	Membrane permeability defined by TA-polyelectrolyte complexation
Pore size *vs.* small molecules	Mesh size ≫ molecule size, poor retention	Tuneable with number of bilayers and post-processing treatments[31]	Nanoscale membrane with effective retention across chemistries, sustainable release
Water consumption	Low to moderate	Very high (10–20 deposition/wash cycles)	Low (single washing step)
Energy demand	Can require heating or long reaction times	Low to moderate	Lower time and energy requirements
Process complexity	Usually one-step, but limited tunability; size-dependent molecular diffusion rates	Highly complex, multistep assembly; loss of cargo during capsule preparation	Simple workflow, two-step process
Mechanical stability	Soft, prone to swelling, however with good stability but at cost of covalent crosslinking	Usually flexible, transparent, rich in water and easily tailored[32]	Tuneable, densified membrane with high robustness
Performance with small hydrophilic molecules	Generally poor, burst release profiles	Achievable at high bilayer counts and using specific polymers, limited scalability	Strong retention independently of molecule chemistry; scalable
Scalability	Excellent	Poor (labour- and time-consuming)	Excellent – easy adaptation to different capsule sizes with similar molecular release profiles

All-aqueous structures *versus* organic solvent-based drug delivery systems (DDSs). Conventional particulate DDSs, widely used in the clinic, are frequently based on water-insoluble synthetic polymers such as polylactic acid (PLA), poly(caprolactone) (PCL) and poly(lactic-*co*-glycolic acid) (PLGA), typically processed using organic solvents to ensure polymer dissolution and particle formation.[33,34] Although these systems enable sustained release profiles and mitigation of burst effects through architectonic control of microparticles and their aggregation into tablets,[35] their fabrication often relies on volatile organic solvents and energy-intensive steps, raising environmental and safety concerns. Residual solvent toxicity and downstream purification requirements further contribute to the ecological footprint of such formulations. In contrast, hydrogels and other structures prepared in all-aqueous environments have been highlighted as promising alternatives capable of reducing the environmental burden associated with pharmaceutical manufacturing.[36,37] TA-coated liquid-core capsules presented herein are fabricated entirely in aqueous media, under mild conditions, without the use of organic solvents or toxic crosslinkers.

All-aqueous liquid-core capsules compared to continuous hydrogels. Hydrogels have emerged as versatile aqueous-based DDSs due to their high-water content, cytocompatibility, and structural similarity to native tissues.[3,38,39] Their three-dimensional crosslinked networks can effectively retain macromolecules with hydrodynamic sizes exceeding the hydrogel mesh size (Fig. 1c),[6,40] while small drugs tend to rapidly diffuse into the medium. Strategies to overcome the latter limitation have primarily relied on tailoring drug–polymer interactions, either *via* covalent conjugation[38] or physical adsorption mechanisms.[33,41–43] While effective, these approaches may increase formulation complexity and restrict the number of polymer–molecule combinations. In contrast, a liquid-core capsule enables efficient encapsulation of small drugs, whereas the surrounding polymeric membrane, further functionalized with tannic acid, acts as a controllable permeability barrier. The polyphenolic coating introduces additional diffusional resistance and promotes reversible supramolecular interactions (*e.g.*, hydrogen bonding and hydrophobic interactions) with small molecules, thus reducing burst release without requiring permanent chemical modification of the drug.

All-aqueous liquid-core capsules compared to conventional LbL and gel-in-gel systems. Multi-compartmentalized hydrogel-in-hydrogel devices[34] and layer-by-layer (LbL) assembled capsules[35,39,40] represent established strategies to modulate drug release under aqueous conditions. The LbL technique, based on the alternate deposition of oppositely charged polymers onto degradable or leachable templates, enables fine control over shell thickness and composition and has been widely applied to load and sustain the release of hydrophilic and hydrophobic compounds.[33,44,45] However, LbL assembly is inherently multistep and time-consuming, typically requiring repeated immersion and rinsing cycles in large volumes of aqueous solutions. Moreover, prolonged exposure of drug-loaded templates to aqueous media during layer deposition may promote premature drug diffusion, compromising encapsulation efficiency unless equilibrium conditions with excess drug are maintained.[33] Gel-in-gel approaches, while effective in creating additional diffusion barriers, also increase structural complexity and processing time.[34] In contrast, the tannic-acid-coated liquid-core capsules described in this work rely on a simplified aqueous fabrication route, where the drug is confined within a liquid core and a single polyphenol-based coating step is employed to tailor drug diffusion kinetics. This

Open Access Article. Published on 06 May 2026. Downloaded on 6/20/2026 10:08:09 AM.
This article is licensed under a Creative Commons Attribution 3.0 Unported Licence.

strategy reduces processing steps, water consumption, and potential drug loss during assembly, while maintaining the ability to regulate small-molecule diffusion.

Assessment of small molecule interactions and diffusion through capsules' membranes

The ability of capsules to minimize or slow down the loading of small molecules with different chemical properties was explored with two additional model molecules besides MB and AR: a zwitterionic molecule, Fast Green (FG, 809 Da)-, and a fully neutral molecule, PEG labelled with FITC (PEG-FITC, 739.4 Da). The capsules were immersed in solutions of the four different dyes to determine the effect of varying pH of the solutions (pH 7.4 in PBS and pH 4 in acetate buffer). The colour of the capsules was inspected after 1 hour immersion, and their liquid core was also inspected after mechanical disruption with a scalpel.

The interactions of the dyes with untreated control capsules and their TA-treated counterparts were assessed by visual inspection of the outer membrane (Fig. 2 and Fig. S5, SI). In non-treated capsules, a dependency on the pH of the dye solution – either at pH 4 or 7 – proved relevant, especially for MB (pK_a ~3.8 (ref. 46)) and AR (pK_a ~8–11 (ref. 46)). Although interactions with the polyelectrolyte membrane were observed for all conditions, with all tested dyes, MB tended to adsorb in higher quantities to the membranes at pH 4, while AR showed an opposite tendency, adsorbing more at pH 7.4. Given the weak polyelectrolyte character of EPL and ALG[17] and the charge features of the dyes,[7] the tendencies in the interactions of AR and MB dyes cannot be explained only by electrostatic preferential interactions. Instead, the results suggest that additional weak interactions, such as hydrogen bonding or hydrophobic effects, play a significant role. Consistent with these observations, zwitterionic FG (pK_a ~3.11 and ~8.9 (ref. 47)) and neutral mPEG-FITC showed relatively high adsorption to the membranes in solutions at both pH 4 and 7.4.

The treatment of capsules with TA led to significant differences in the propensity of different dyes to interact with the capsule membranes (Fig. 2). At pH 7.4, a visible reduction of the interaction of MB, AR and mPEG-FITC was observed. Also, as a general trend, dyes tended to adsorb in more abundance to capsule walls under pH 4 conditions. The hydroxyl groups of TA are known to display different oxidation states depending on pH: at pH 4, the hydroxyl groups tend to be protonated, conferring a general neutral charge to the polyphenol.[18] Therefore, the interactions established between TA and the polyelectrolytes are expected to be mainly driven by H-bonds and hydrophobic bonds.[20] In contrast, at pH 7.4, the hydroxyl groups tend to deprotonate, acquiring a negative charge, which could allow the establishment of additional electrostatic interactions with other molecules. Thus, at pH 7.4, besides hydrogen bonds, TA molecules probably electrostatically interacted with the positively charged amine groups of EPL, promoting the TA wrapping around such polyelectrolytes, possibly forming a more compact network (Fig. 1A).

Overall, the post-treatment of capsules with TA led to an almost complete impermeabilization of the capsules at pH 4 for both AR and MB, but not for FG. At pH 7.4, however, an apparent complete impermeabilization (no dye detected in the liquid core after capsule burst) was observed (Fig. 2) for AR and MB. For FG, a noticeable decrease in permeability was also observed at pH 7.4 after capsule rupture. The unspecific interaction of TA with MB was previously reported to occur through electrostatic and/or π–π interactions.[48] Given that in the case of MB and FG, visible adsorption of the dyes occurred in the membranes (in the case of MB in localized dye-dense patterns), we performed a subsequent study to elucidate the dependence of the impermeabilization phenomenon on the formation of dye-TA complexes in the membranes. Interestingly, even for the lowest TA concentration (0.1%), the permeation of all dyes was prevented for all conditions after a 1-hour immersion at pH 7.4. Observational experiments were also performed to better characterize the affinity and tendency for the formation of aggregates between free dyes and solubilized TA. Of all dyes, MB immediately formed easily detected precipitates (Fig. S6A, SI), while this phenomenon was not observed for the other dyes. Surprisingly, MB interactions with the membrane showed a proportional decrease with increasing concentration of TA used to treat the capsules, indicating that not only the amount of TA could lead to the entrapment of MB in localized patterns, but also its conformation (or of denser TA–TA complexes) may be important to prevent the adsorption of MB (Fig. S6B and C, SI). This result suggests that TA is mostly bound to the polyelectrolyte complexed membrane, and not available in its free form to interact with its most favourable interacting dye (MB). FG showed a similar tendency (Fig. 2), although differences were more difficult to detect, suggesting that the interaction of FG with the membrane is not as sensitive to the TA content and/or conformation as MB. An opposite effect was observed for AR, with visually detected higher dye retention in the membranes for higher concentrations of TA.

Development of encapsulation strategies for different dyes

Initial attempts to load small molecules in a single step during polyelectrolyte complexation resulted in substantial loss of cargo to the surrounding bath phase. To improve loading efficiency, the encapsulation protocols were subsequently optimized. Additionally, processing conditions were adjusted to prevent or minimize the precipitation of small molecules upon contact with tannic acid (TA). Two main routes were established:

Route (A): After capsule manufacture, the loading of small molecules was performed by capsule incubation in dye solutions for 1 h. During the subsequent TA post-treatment step, the TA solution also incorporated with the same concentration of dissolved dye to minimise dye release from the liquid core of the capsules into the surrounding bath phase (Fig. 3A). Due to the formation of aggregates, the application of this method was not feasible for the encapsulation of MB and mPEG-FITC. AR and FG could be successfully encapsulated using this strat-

 This journal is © The Royal Society of Chemistry 2026

Open Access Article. Published on 06 May 2026. Downloaded on 6/20/2026 10:08:09 AM.
This article is licensed under a Creative Commons Attribution 3.0 Unported Licence.

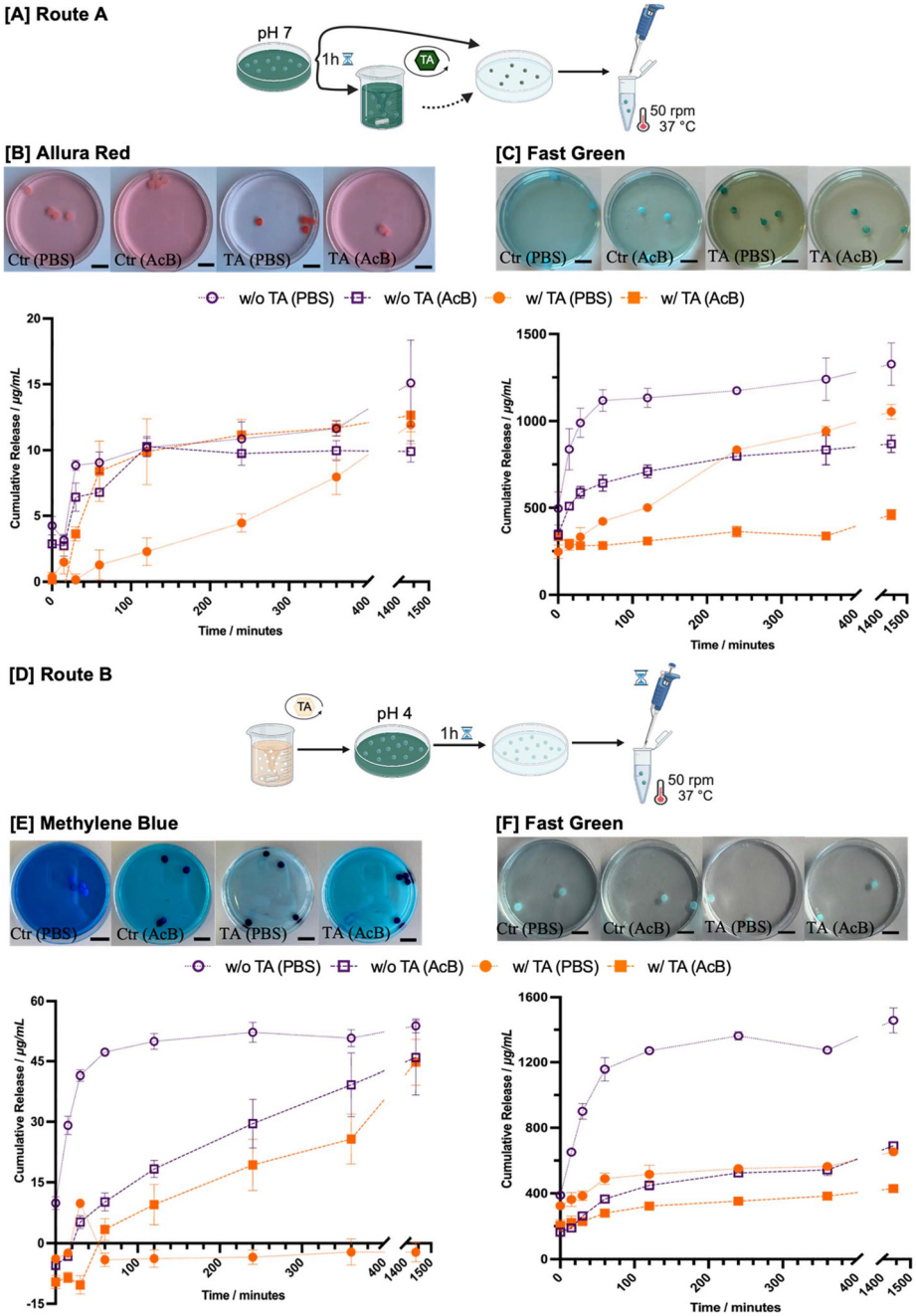

Fig. 3 Release profiles of different dyes from capsules with and without TA post-treatment, under distinct release conditions. [A] Schematic representation of the procedure followed to test the dye release from the capsules, according to route A from the "Results and discussion" section. [B] Release of AR in phosphate buffered saline (PBS) (pH 7.4) and in acetate buffer (AcB) (pH 4) from capsules with and without TA post-treatment, after exposure to each buffer overnight. Scale bar: 1 cm. The graph present in the bottom shows the release of AR from capsules, with and without TA post-treatment, and an excess of dye after dye loading (route A) at pH 7.4. [C] Release of FG in PBS (pH 7.4) and in AcB (pH 4) from capsules with and without TA post-treatment, after exposure to each buffer overnight. Scale bar: 1 cm. The graph present in the bottom shows the release of FG from capsules, with and without TA post-treatment, and an excess of dye after dye loading (route A) at pH 7.4. [D] Schematic representation of the procedure followed to test the dye release from the capsules, according to route B from the "Results and discussion" section. [E] Release of MB in PBS (pH 7.4) and in AcB (pH 4) from capsules with and without TA post-treatment, after exposure to each buffer overnight. Scale bar: 1 cm. The graph present in the bottom shows the release of MB from capsules post-treated with TA before dye loading (Route B) at pH 4. [F] Release of FG in PBS (pH 7.4) and in AcB (pH 4) from capsules with and without TA post-treatment, after exposure to each buffer overnight. Scale bar: 1 cm. The graph present in the bottom shows the release of FG from capsules post-treated with TA before dye loading (route B) at pH 4. Release studies were conducted at 37 °C under agitation (50 rpm), using, for the release, PBS at pH 7.4 and AcB at pH 4, to simulate physiological conditions. In all graphs, pointed purple lines (-●-) indicate control capsules released in PBS; dashed purple lines (-●-) correspond to control capsules released in AcB; pointed orange lines (-●-) represent TA-treated capsules released in PBS; and dashed orange lines (-●-) denote TA-treated capsules in AcB. Data are presented as mean ± SD (n = 2 to 3).

Open Access Article. Published on 06 May 2026. Downloaded on 6/20/2026 10:08:09 AM.
This article is licensed under a Creative Commons Attribution 3.0 Unported Licence.

egy (Fig. 3B and C). The results obtained with this method must also be carefully analysed, given that the encapsulated fractions of dye may be composed of dissolved dye, or dye-TA nanoparticles. The steps of the strategy are depicted in Fig. 3A.

Route (B): Direct dye loading into TA-treated capsules at pH 4. In this strategy, the capsules were treated with TA using the optimized protocol and thoroughly washed with PBS to eliminate non-reacted TA. The loading of dyes was then performed at pH 4, given the previous permeability results showing that capsules are more permeable at this pH, when compared to pH 7.4 (Fig. 3D). Optimization results showed that the permeability of the capsules when put back in a solution of PBS at pH 7.4 was again decreased compared to pH 4, although a loss of efficiency was observed (the capsules were no longer impermeable to any of the dyes). This result suggests that during the "weakening" period at pH 4, TA may be released from the capsules or lose its initial arrangement in the capsule walls, which made it compatible with the almost total impermeability observed in the original capsules. This strategy was successfully implemented for the loading of MB and FG (Fig. 3E and F). Of note, the zwitterionic dye FG could be loaded to the capsules using both strategies. This strategy minimizes the probability of interaction between free TA and the dye, likely leading to higher fractions of free dye encapsulated in the capsule's core (when compared to route A). The steps of route B are depicted in Fig. 3D.

Although strategies to enable the loading of MB, AR and FG into the capsules could be formulated, the complex phenomena mediating the different behaviors of the dyes seem to be partially attributed to the presence of charges in the loaded molecules, and their interactions with the polyelectrolyte membrane. To better understand membrane properties, a neutral molecule, polyethylene glycol (PEG)-, labelled with neutral fluorescein isocyanate (~800 Da for mPEG-FITC) was used. The capsules were studied during drug loading at pH 7.4, following the described method:

Route (C): Given that mPEG-FITC tended to precipitate and lose its fluorescence at pH 4, the loading of this dye was performed in the capsules for 1 hour at pH 7.4, and TA was added afterwards (Fig. 4A). Optimizations showed that the permeability of the capsules to this molecule after treatment with TA was reduced in comparison with the control counterparts, although equilibrated amounts of the dye could be observed in the inner and outer liquids after this time.

Release studies of dyes loaded in TA-treated capsules

After the loading of the molecules, their release into PBS (pH 7.4) and acetate buffer (pH 4) was evaluated at 37 °C under agitation while maintaining sink conditions. The release of AR from TA-treated capsules showed a controlled release of the dye for 24 hours at pH 7.4 (Fig. 4B). Both untreated samples at pH 4 and 7.4, as well as TA-treated capsules at pH 4 present a burst-like release profile, reaching a plateau in approximately 2 hours. MB release showed a different trend, with a close-to-null release for 24 hours on TA-treated capsules at pH 7.4 (Fig. 4E). In contrast, non-treated capsules led to a fast burst release-mediated diffusion of MB. Both TA-treated and control capsules at pH 4 enabled a close-to-linear controlled release of MB for 24 hours, suggesting that indeed a decrease in pH from 7 to 4 tends to permeabilize TA-treated capsules; also, the decrease of pH in untreated capsules decreases their permeability to MB, although this effect was not visible for AR. Interestingly, the effect of pH decrease in untreated capsules was also observed for zwitterionic FG (Fig. 4C and F), encapsulated using either route A or B, suggesting that the slower diffusion of small dyes at pH 4 may be related to the existence of positive charges in the loaded molecules. The loading of FG by the two different methods led to similar release profiles for all tested conditions, suggesting that the putative/facilitated generation of TA-FG complexes in the route B methodology should not interfere with the release profile of the molecule in a relevant manner. Overall, a very low release of FG was observed at pH 4 in TA-treated capsules, with a mass of *ca.* 200–250 μg released right after washing, and a stagnant release profile for a course of 24 hours. TA-treated capsules at pH 7.4 and untreated capsules at pH 4 led to slightly higher release of FG with higher released masses with route A compared to the route B methodology. Similarly to what was observed for other molecules, untreated capsules at pH 7.4 led to a fast diffusion of FG.

For mPEG-FITC, the effectiveness of the loading strategy was assessed through analysis of the inner liquid core of the capsules. Using a needle, the inner liquid of the capsules was collected at specific timepoints, and fluorescence was quantified using a microplate reader. The increase of fluorescence in the inner part of the capsules was achieved within 3 hours for the control (non-coated) capsules, while for TA-treated capsules, the equilibrium between the outer and inner concentration of mPEG-FITC took 6 hours (Fig. 4B and C). After loading, the release of the cargo was assessed, with TA-treated samples showing a much slower release profile, closer to a linear trend. The control (non-treated samples) showed a typical burst release until ~100 minutes, followed by a stable and controlled release up until 24 hours, in which both conditions equalled their cumulative released mass (Fig. 3A). The liquid content of the capsules was also inspected during the same period. The concentration of mPEG-FITC inside the untreated capsules matched the release profile in an inverse manner (Fig. 4B). Interestingly, qualitative observations suggested that a fraction of the dye was retained in the capsule membrane. To further inspect this behaviour, fluorescence microscopy images were acquired, using mPEG-FITC-labelled molecules, after inducing the collapse of millimetric capsules and washing the remaining membrane structures. The presence of residual fluorescence localized at the membrane region indicated that part of the dye remained associated with the polymeric network (Fig. 4E and F). Such behavior may arise from non-specific interactions between the dye molecules and the membrane components, potentially involving electrostatic interactions or hydrogen bonding. These observations motivated a more detailed investigation into whether TA primarily acts as a dye-binding retentive agent or modulates

 This journal is © The Royal Society of Chemistry 2026

Open Access Article. Published on 06 May 2026. Downloaded on 6/20/2026 10:08:09 AM.
This article is licensed under a Creative Commons Attribution 3.0 Unported Licence.

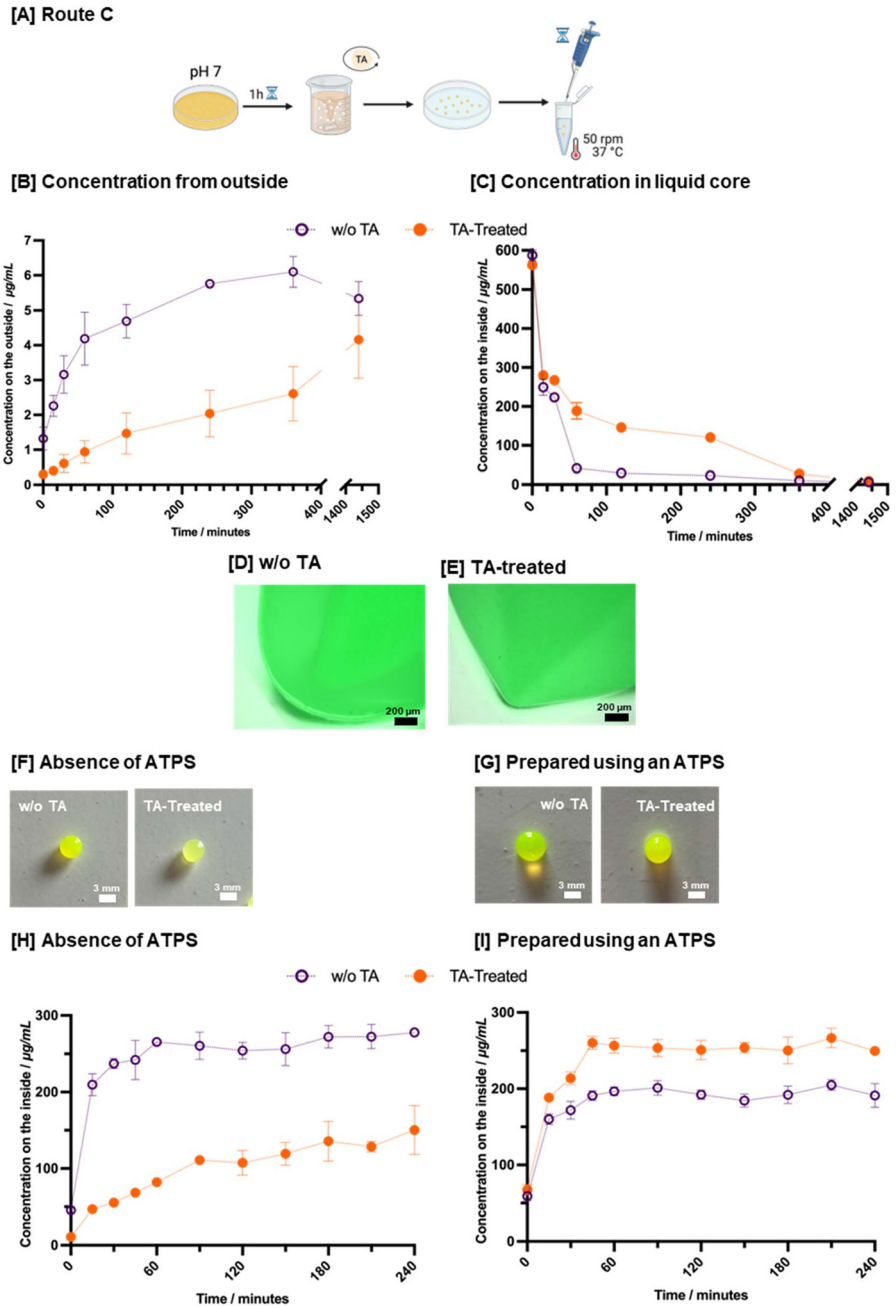

Fig. 4 Release profiles of mPEG-FITC from millimetric-sized capsules with and without TA post-treatment. [A] Schematic representation of the procedure followed to test the dye release from the capsules, according to route C. [B] Concentration of mPEG-FITC on the outside of the capsule over time. The release profiles are shown for both capsules without (purple) and with (orange) TA post-treatment, following dye loading at pH 7.4. The data were collected from the surrounding medium over the course of the experiment. [C] Concentration of mPEG-FITC within the liquid core of the capsule over time. The release profiles are shown for both capsules without (purple) and with (orange) TA post-treatment, following dye loading at pH 7.4. Measurements were made after draining the surrounding medium and cutting the capsule. [D] Non-treated capsules and [E] TA-treated capsules. Fluorescence microscopy images of millimetric-sized capsules, before and after bursting, after 1 hour of immersion in mPEG-FITC, showcasing partial retention or adsorption of the dye in the polymeric network even after a washing step. [F] Macroscopic images of capsules in the absence of ATPS, showing the appearance of both control and TA-treated capsules loaded with mPEG-FITC. [G] Macroscopic images of capsules prepared using an ATPS, showing improved dye retention in TA-treated capsules compared to untreated ones. [H] Quantification of mPEG-FITC retention in the absence of ATPS, showing the concentration inside the capsules over time. [I] Quantification of PEG-FITC retention in capsules prepared using an ATPS, showing enhanced mPEG-FITC retention in TA-treated capsules (orange line) compared to untreated ones (purple line). Release studies were conducted at RT, and the capsules were immersed in a mPEG-FITC dye solution in order to evaluate membrane permeation. In all graphs, pointed purple lines (●) indicate control capsules released in PBS; and pointed orange lines (●) represent TA-treated capsules released in PBS. Data are represented as mean ± SD (n = 3).

Open Access Article. Published on 06 May 2026. Downloaded on 6/20/2026 10:08:09 AM.
This article is licensed under a Creative Commons Attribution 3.0 Unported Licence.

membrane permeability by promoting a reduction in the effective molecular weight cut-off (MWCO). Capsules prepared using an ATPS (dextran/PEG) were treated with TA and later assessed for their ability to impair or slow down the entrance of mPEG-FITC. Those untreated capsules were previously shown to enable the rapid permeation of molecules up to 150 kDa.[13] Overall, we observed that even after TA treatment, capsules prepared in the presence of ATPS still led to the rapid diffusion of this neutral small molecule (Fig. 4G and H). This result shows that, while TA-dye binding may play a role in preventing the rapid leakage of small molecules from the membranes, the TA coating seems to be only effective when applied to capsules with low initial MWCO (in this case, <10 kDa). Overall, these results show that TA modification, and molecular binding to the membrane, is not sufficient to enable the slow release of small molecules.

Assessment of capsule miniaturization on the performance of low-permeability core–shell systems

Liquid-core capsules may be useful in several applications that may require the processing of small capsules, for example, to be applied in different body locations for drug delivery, such as defect-localized settings with challenging geometries. In this scope, micrometric-sized capsules were produced by electrodynamic atomization, reaching diameters of *ca.* 600 μm (Fig. 5A–C). With this approach, we aimed at understanding whether the coating with TA could provide a universal effect on the regulation of the diffusion of encapsulated dyes regardless of the capsule size. The release of mPEG-FITC from miniaturized capsules was assessed by fluorescence microscopy. The overall detected fluorescence was plotted over 5 hours (Fig. 5D), and the liquid core of those structures was also assessed by bursting capsules at specific time points and acquiring images of the released liquid. Therefore, similar data to the one shown in Fig. 4D (collected in standard molecule release assays) were collected with an image-based approach. In the initial timepoint, the analysis of non-ruptured capsules showed higher fluorescence values for TA-treated samples (Fig. 5E and F). The analysis of the liquid core after rupture at the same timepoint corroborated that, indeed, TA-treated samples were overall richer in mPEG-FITC. This suggests that, for such small capsules, the initial washing steps (before the release study starts) probably lead to a relevant loss of mPEG-FITC in untreated capsules. The decrease in fluorescence over time on control capsules was fast and happened with an apparent burst release-like profile. On their turn, TA-treated capsules led to a more close-to-linear decrease in the fluorescence of the intact capsules (Fig. 5E), in a similar way to the results on millimetric-sized capsules (Fig. 4B). The analysis of the fluorescence in the liquid cores (Fig. 4C and 5F) showed a similar trend to the one observed for millimetric capsules. The modulating profile of TA in micrometric capsules was also corroborated using AR in traditional molecule release assays (Fig. 5G).

Assessing TA-modified capsules: high-loader encapsulation and tolerance to organic solvents

To further evaluate the versatility of the capsule membrane system, tests were conducted to investigate its performance under higher payload conditions. Capsule geometry stability was first assessed using high concentrations of the negatively charged Allura Red (AR) (Fig. S7, SI). Of note, AR concentrations above 2.5 mg mL^{-1} led to visible loss of capsule integrity (Fig. S7, SI), likely due to competition between the dye's negative charges and polyelectrolyte–polyelectrolyte interactions within the membrane. For this reason, release studies were performed only with AR concentrations below this threshold. The encapsulation process was successfully replicated with a 1 mg mL^{-1} solution and 2 mg mL^{-1} solution (Fig. S8, SI), corresponding to approximately 20-fold higher concentrations than initially reported. Sustained release profiles were obtained for TA-modified capsules at these higher concentrations. Tests with the neutral charge mPEG-FITC were then performed and, in that case, high dye concentrations did not compromise capsule integrity or stability (Fig. S9, SI). Of note, the limit concentration of 10 mg mL^{-1} was tested, given that for higher concentrations precipitation was observed.

The use of TA-modified capsules depends on the ability of soluble molecules to enter the inner region of the construct. Even with the proven ability of capsules to withstand more concentrated dye encapsulation and controlled release, this limitation may still comprise substantial drawbacks in the application of this technology, for example, in the pharmaceutical industry, where high concentrations of drugs are usually sought, and most drugs are hydrophobic in nature. A pilot study comprising the incorporation of organic solvents in the loading solution was performed to expand the possible applications of the developed methodology. Non-treated and TA-treated capsules withstood 10 minutes of immersion in ethanol (Fig. S10 and S11, SI) at various concentrations without visible loss of membrane integrity, showcasing shape recoverability after rehydration in distilled water. Of note, TA-treated capsules retained their repellence to MB regardless of ethanol concentration, indicating that the TA coating remained associated with the membrane structure (Fig. S11, SI). Inspection of capsules' cores revealed increased MB entry in ethanol-treated capsules compared to unexposed controls; however, penetration remained lower than that in non-TA-treated capsules (up to 50% v/v ethanol). These results suggest that, despite partial damage and the probably partial loss of TA, the reduced permeability conferred by TA treatment may be exploited in the future for controlled release studies. In contrast, DMSO (Fig. S12 and S13, SI) exposure led to visible loss of MB repellence in TA-treated capsules under all tested conditions, although MB penetration into the capsule core also remained lower than that in non-TA-treated capsules, up to 50% v/v DMSO, reflecting partial retention of TA-induced barrier properties (Fig. S14).

Overall, these findings demonstrate that the capsule system maintains functional integrity across a wide range of payloads and environmental conditions. Moreover, TA treatment

 This journal is © The Royal Society of Chemistry 2026

Open Access Article. Published on 06 May 2026. Downloaded on 6/20/2026 10:08:09 AM.
This article is licensed under a Creative Commons Attribution 3.0 Unported Licence.

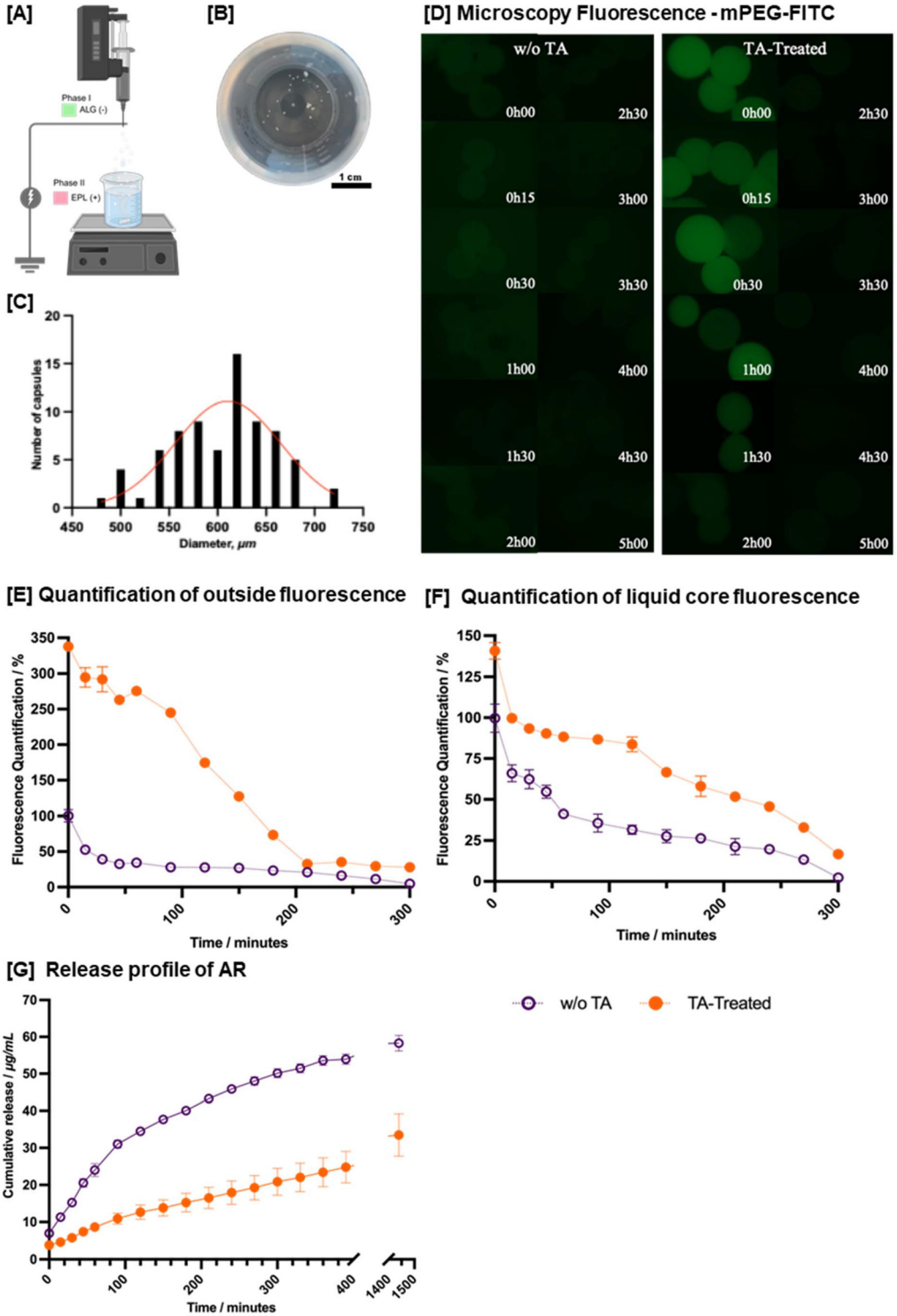

Fig. 5 Release profiles of mPEG-FITC from micrometric-sized capsules with and without TA post-treatment. [A] Schematic representation of an electrospray ionization source. [B] Top view of the micrometric capsules. [C] Size distribution of micrometric capsules showing the diameter (in μm) of capsules used in the experiments, with a peak at around 620 μm. [D] Microscopy fluorescence images of mPEG-FITC in micrometric capsules at different time intervals. Images show capsules without TA (left) and with TA treatment (right), with time points of 0 h, 0 h 15, 0 h 30, 0 h 45, 1 h, 1 h 30, 2 h, 2 h 30, 3 h 00, 3 h 30, 4 h, 4 h 30 and 5 h 00. [E] Quantification of outside fluorescence over time. Fluorescence levels in the surrounding medium are shown for both micrometric capsules without (purple) and with (orange) TA post-treatment. [F] Quantification of liquid core fluorescence over time. Fluorescence levels inside the capsule core are shown for both micrometric capsules without (purple) and with (orange) TA post-treatment. [G] Release profile of AR encapsulated in micrometric capsules. Release studies were conducted at 37 °C under agitation, using PBS for the release, at pH 7.4, to simulate physiological conditions. In all graphs, pointed purple lines (●) indicate control capsules released in PBS, and pointed orange lines (●) represent TA-treated capsules' release in PBS. Data are represented as mean ± SD (n = 3).

Open Access Article. Published on 06 May 2026. Downloaded on 6/20/2026 10:08:09 AM.
This article is licensed under a Creative Commons Attribution 3.0 Unported Licence.

enhances resilience against solvent-induced permeability changes, and the system can accommodate higher concentrations of both hydrophilic and moderately soluble molecules, highlighting the versatility and potential of this platform for complex encapsulation and controlled release scenarios.

While exposure to aqueous saline and organic solvents provides an initial indication of the structural robustness of the developed capsules, a systematic evaluation in biologically relevant environments containing factors such as competitive binding species and enzymes is identified as an important direction for future work.

Modelling of diffusion release from polymeric capsules

The release behaviour of encapsulated molecules from polymeric capsules was systematically analysed using several mathematical kinetic models to obtain insight into the underlying molecular transport mechanisms. The experimental release profiles were fitted to different models, including zero-order, first-order, Higuchi, Korsmeyer–Peppas and Weibull equations. Overall, the Weibull model provided the best description of most of the experimental datasets, with coefficients of determination (R^2) typically higher than 0.90 (Table S2). The Weibull equation can be expressed as $M(t) = 1 - \exp(-(t/b)\hat{}c)$, where b represents the scale parameter related to the characteristic time of the release process, while c reflects the shape of the release curve and therefore provides information about the dominant transport mechanism. Specifically, $c \leq 0.75$ is generally associated with Fickian diffusion, $0.75 < c < 1$ suggests combined diffusion–relaxation mechanisms, $c \approx 1$ indicates exponential or first-order release kinetics, and $c > 1$ suggests sigmoidal or more complex transport behaviour.[49]

The analysis of the kinetic parameters revealed distinct release behaviours depending on both the encapsulated molecule, the capsule coating and the surrounding medium. For AR-loaded capsules, the Weibull model consistently described the release behaviour across different conditions. Control capsules in PBS displayed a shape parameter of $c = 0.40$, which is characteristic of Fickian diffusion through a hydrated polymeric matrix. In contrast, TA-treated capsules exhibited a markedly higher value ($c = 1.41$), indicating a transition toward sigmoidal or more complex release behaviour. A similar tendency was observed in acetate buffer, where c increased from 0.99 in control capsules to 2.21 in TA-treated capsules. Concomitantly, the scale parameter b increased significantly upon TA treatment, reflecting slower release kinetics. In PBS, b increased from 124.5 for control capsules to 365.2 after TA treatment, while in acetate buffer, the value increased from 38.8 to 51.5. These results suggest that the TA coating substantially increases resistance to molecular diffusion.

For MB-loaded capsules, the kinetic behaviour differed slightly. In PBS, the release profile of control capsules was better described by a first-order model ($k = 0.05$), suggesting a concentration-dependent release mechanism. In contrast, release from capsules in acetate buffer was again best fitted by the Weibull model, with $c = 1.20$ for control capsules and $c = 1.58$ for TA-treated capsules, both indicating non-Fickian transport behaviour. The relatively high values of the scale parameter ($b = 218.7$ and 369.3, respectively) suggest slower diffusion dynamics compared to AR systems.

For FG-loaded capsules, most datasets were also well described by the Weibull model across both release routes tested. Control capsules frequently exhibited shape parameters below unity (*e.g.*, $c = 0.30$ to 0.71), consistent with diffusion-controlled release. Upon TA treatment, the release behaviour showed notable changes depending on the route and medium. For example, in PBS route A, the b parameter increased dramatically from 12.2 in control capsules to 163.7 in TA-treated capsules, indicating a strong retardation of molecular diffusion. In acetate buffer under route A conditions, the release from TA-treated capsules followed a zero-order model ($k \sim 0.12$), suggesting a near-constant release rate over time. In contrast, route B datasets remained well described by Weibull kinetics, although with altered parameters reflecting slower release and modified transport mechanisms.

The release behaviour of mPEG-FITC further supported the influence of TA treatment on diffusion dynamics. Both control and TA-treated capsules followed Weibull kinetics with excellent goodness of fit (R^2 up to 0.999). Notably, TA treatment produced a dramatic increase in the scale parameter, from $b = 42.2$ in control capsules to $b = 535.6$ in TA-treated capsules, indicating a strong reduction in diffusion rate. However, the shape parameter remained relatively similar ($c \sim 0.69$ in both cases), suggesting that the fundamental release mechanism remained predominantly diffusion-driven despite the slower kinetics. Comparable Weibull behaviour was observed for liquid-core capsules and saturated solution systems, although variations in b and c reflected the influence of molecular concentration and core structure on transport dynamics.

Finally, AR release from saturated solutions and miniaturized capsules also followed Weibull kinetics with excellent fits ($R^2 \sim 0.99$). For miniaturized capsules, TA treatment again resulted in a substantial increase in the scale parameter ($b = 143.7$ for controls *vs.* 362.8 for TA-treated capsules), confirming the consistent diffusion-limiting effect of the polyphenol coating across different capsule architectures.

Overall, the systematic shifts in the Weibull parameters suggest that TA treatment modifies both the rate and mechanism of molecular transport across the capsule membrane. These observations support a material-based hypothesis in which TA interacts with the Alg/EPL membrane, likely inducing partial densification and reducing the effective mesh size of the polymeric network, while potentially forming a thin interfacial barrier layer. Such structural changes would slow molecular diffusion and, in some cases, alter the release mechanism from simple Fickian transport to more complex sigmoidal or relaxation-mediated behaviours.

Conclusions

We have demonstrated that liquid core capsules fabricated in all-aqueous environments can be effectively modified to

 This journal is © The Royal Society of Chemistry 2026

Open Access Article. Published on 06 May 2026. Downloaded on 6/20/2026 10:08:09 AM. This article is licensed under a Creative Commons Attribution 3.0 Unported Licence.

achieve the controlled release of small molecules with diverse chemical properties. Release studies under acidic and neutral pH conditions confirmed that, while kinetics depend on the molecular charge and structure, tunable release profiles are attainable for positively charged, negatively charged, zwitterionic, and neutral molecules. Kinetic modulation studies suggest that the diffusion-mediated release observed in untreated capsules is modified to more complex release mechanisms in the presence of the TA treatment. The capsules showed partial resistance and preserved functionality upon contact with organic solvents, paving the way for more complex encapsulation studies in the future. Furthermore, the miniaturization of the capsules *via* electrospraying was successfully performed, and the role of the TA coating in regulating molecular release was validated in these downsized structures. By enabling the rapid and safe fabrication of capsules under mild and entirely aqueous conditions, this technology minimizes solvent wastage and energy consumption, aligning closely with the core principles of green chemistry. Together, our findings highlight the versatility of all-aqueous capsule systems and provide a platform for the rational design of miniaturized carriers for delivery applications.

Conflicts of interest

There are no conflicts to declare.

Data availability

All data supporting the findings of this study are available within the article and its supplementary information (SI). Supplementary information is available. See DOI: https://doi.org/10.1039/d6gc01588c.

Acknowledgements

This work was supported by the project Suspharma – Merging sustainable and digital chemical technologies for the development of greener-by-design pharmaceuticals (HORIZON-HLTH-2021-IND-07-101057430) and the Portuguese Foundation for Science and Technology (FCT) with the project "CellFi" PTDC/BTM-ORG/3215/2020 (https://doi.org/10.54499/PTDC/BTM-ORG/3215/2020). This work was also developed within the scope of the project CICECO – Aveiro Institute of Materials, UID/50011/2025 & LA/P/0006/2020 (https://doi.org/10.54499/LA/P/0006/2020), financed by national funds through the FCT/MCTES (PIDDAC).

References

1 D. Bora, Small Molecule Drug Discovery Market Size, Demand, Report to 2033, 2024https://straitsresearch.com/report/small-molecule-drug-discovery-market#keyplayeroverview.
2 A. M. Silva, C. Martins-Gomes, S. S. Ferreira, E. B. Souto and T. Andreani, Molecular Physicochemical Properties of Selected Pesticides as Predictive Factors for Oxidative Stress and Apoptosis-Dependent Cell Death in Caco-2 and HepG2 Cells, *Int. J. Mol. Sci.*, 2022, **23**, 8107, DOI: 10.3390/ijms23158107.
3 A. M. Vargason, A. C. Anselmo and S. Mitragotri, The evolution of commercial drug delivery technologies, *Nat. Biomed. Eng.*, 2021, **5**, 951–967.
4 S. M. Rodrigues, A. Avellan, D. Salvador, S. Rodrigues, M. Miranda and B. Morais, *et al.*, *Nanofertilizers—synthesis, advantages, and the current status*, in *Nano-Enabled Sustainable and Precision Agriculture*. Elsevier, 2023, pp. 43–77.
5 M. J. Mitchell, M. M. Billingsley, R. M. Haley, M. E. Wechsler, N. A. Peppas and R. Langer, Engineering precision nanoparticles for drug delivery, *Nat. Rev. Drug Discovery*, 2021, **20**, 101–124.
6 J. Li and D. J. Mooney, Designing hydrogels for controlled drug delivery, *Nat. Rev. Mater.*, 2016, **1**, 16071, DOI: 10.1038/natrevmats.2016.71.
7 B. S. Neves, R. C. Gonçalves, J. F. Mano and M. B. Oliveira, Controlling the diffusion of small molecules from matrices processed by all-aqueous methodologies: towards the development of green pharmaceutical products, *Green Chem.*, 2024, **26**, 4417–4431.
8 S. A. Abouelmagd, N. H. Abd Ellah, O. Amen, A. Abdelmoez and N. G. Mohamed, Self-assembled tannic acid complexes for pH-responsive delivery of antibiotics: Role of drug-carrier interactions, *Int. J. Pharm.*, 2019, **562**, 76–85.
9 TYLENOL®, Extra Strength TYLENOL® Rapid Release Gels, https://www.tylenol.com/products/headache-pain-relief/tylenol-rapid-release-gels.
10 K. T. Campbell, K. Wysoczynski, D. J. Hadley and E. A. Silva, Computational-Based Design of Hydrogels with Predictable Mesh Properties, *ACS Biomater. Sci. Eng.*, 2020, **6**, 308–319.
11 B. G. Amsden, Hydrogel Mesh Size and Its Impact on Predictions of Mathematical Models of the Solute Diffusion Coefficient, *Macromolecules*, 2022, **55**, 8399–8408.
12 D. Choi, K. Gwon, H. J. Hong, H. Baskaran, O. Calvo-Lozano, A. M. Gonzalez-Suarez, *et al.*, Coating Bioactive Microcapsules with Tannic Acid Enhances the Phenotype of the Encapsulated Pluripotent Stem Cells, *ACS Appl. Mater. Interfaces*, 2022, **14**, 27274–27286.
13 R. C. Gonçalves, S. Vilabril, C. M. S. S. Neves, M. G. Freire, J. A. P. Coutinho, M. B. Oliveira, *et al.*, All-Aqueous Freeform Fabrication of Perfusable Self–Standing Soft Compartments, *Adv. Mater.*, 2022, **34**, 2200352, DOI: 10.1002/adma.202200352.
14 X. Huang, L. Tian, Z. Wang, J. Zhang, Y. S. Chan, S. H. Cheng, *et al.*, Bioinspired Robust All-Aqueous Droplet via Diffusion-Controlled Interfacial Coacervation, *Adv. Funct. Mater.*, 2020, **30**, 2004166, DOI: 10.1002/adfm.202004166.

Open Access Article. Published on 06 May 2026. Downloaded on 6/20/2026 10:08:09 AM. This article is licensed under a Creative Commons Attribution 3.0 Unported Licence.

15 M. Oćwieja, Z. Adamczyk and M. Morga, Adsorption of tannic acid on polyelectrolyte monolayers determined in situ by streaming potential measurements, *J. Colloid Interface Sci.*, 2015, **438**, 249–258.
16 J. Siepmann, N. Faisant, J. Akiki, J. Richard and J. P. Benoit, Effect of the size of biodegradable microparticles on drug release: experiment and theory, *J. Controlled Release*, 2004, **96**, 123–134.
17 F. G. Perfeito, S. Vilabril, A. Cerqueira, M. B. Oliveira and J. F. Mano, Spontaneous Formation of Solid Shell Polymeric Multicompartments at All–Aqueous Interfaces, *Adv. Sci.*, 2024, **11**, 2402592, DOI: 10.1002/advs.202402592.
18 X. Liang, K. Cao, W. Li, X. Li, D. J. McClements and K. Hu, Tannic acid-fortified zein-pectin nanoparticles: Stability, properties, antioxidant activity, and in vitro digestion, *Food Res. Int.*, 2021, **145**, 110425, DOI: 10.1016/j.foodres.2021.110425.
19 R. Lu, X. Zhang, X. Cheng, Y. Zhang, X. Zan and L. Zhang, Medical Applications Based on Supramolecular Self-Assembled Materials From Tannic Acid, *Front. Chem.*, 2020, **8**, 583484, DOI: 10.3389/fchem.2020.583484.
20 E. Olaret, J. Ghitman, H. Iovu, A. Serafim and I. C. Stancu, Coatings based on mucin-tannic acid assembled multilayers, Influence of pH, *Polym. Adv. Technol.*, 2020, **31**, 645–653.
21 S. V. Jasemi, H. Khazaei, M. R. Morovati, T. Joshi, I. Y. Aneva, M. H. Farzaei, *et al.*, Phytochemicals as treatment for allergic asthma: Therapeutic effects and mechanisms of action, *Phytomedicine*, 2024, **122**, 155149.
22 R. Abka-khajouei, L. Tounsi, N. Shahabi, A. K. Patel, S. Abdelkafi and P. Michaud, Structures, Properties and Applications of Alginates, *Mar. Drugs*, 2022, **20**, 364.
23 L. Wang, C. Zhang, J. Zhang, Z. Rao, X. Xu, Z. Mao, *et al.*, Epsilon-poly-L-lysine: Recent Advances in Biomanufacturing and Applications, *Front. Bioeng. Biotechnol.*, 2021, **9**, 748976, DOI: 10.3389/fbioe.2021.748976.
24 W. Yan, M. Shi, C. Dong, L. Liu and C. Gao, Applications of tannic acid in membrane technologies: A review, *Adv. Colloid Interface Sci.*, 2020, **284**, 102267.
25 C. Chen, H. Yang, X. Yang and Q. Ma, Tannic acid: A crosslinker leading to versatile functional polymeric networks: A review, *RSC Adv.*, 2022, **12**, 7689–7711.
26 A. Chandra, V. Kumar, U. C. Garnaik, R. Dada, I. Qamar, V. K. Goel, *et al.*, Unveiling the Molecular Secrets: A Comprehensive Review of Raman Spectroscopy in Biological Research, *ACS Omega*, 2024, **9**, 50049–50063.
27 F. Zapata, A. López-Fernández, F. Ortega-Ojeda, G. Quintanilla, C. García-Ruiz and G. Montalvo, Introducing ATR-FTIR Spectroscopy through Analysis of Acetaminophen Drugs: Practical Lessons for Interdisciplinary and Progressive Learning for Undergraduate Students, *J. Chem. Educ.*, 2021, **98**, 2675–2686.
28 P. Anastas and J. Warner *Green Chemistry: Theory and Practice*, Oxford University Press, 2000, DOI: 10.1007/978-981-15-6453-6_84-1.
29 S. Nadine, S. G. Patrício, C. C. Barrias, I. S. Choi, M. Matsusaki, C. R. Correia, *et al.*, Geometrically Controlled Liquefied Capsules for Modular Tissue Engineering Strategies, *Adv. Biosyst.*, 2020, **4**, 2000127, DOI: 10.1002/adbi.202000127.
30 A. Bardow, J. Pérez-Ramírez, S. Sala and L. Vaccaro, Measuring green chemistry: methods, models, and metrics, *Green Chem.*, 2024, **26**, 11016–11018.
31 A. P. R. Johnston, C. Cortez, A. S. Angelatos and F. Caruso, Layer-by-layer engineered capsules and their applications, *Curr. Opin. Colloid Interface Sci.*, 2006, **11**, 203–209.
32 W. Tong, X. Song and C. Gao, Layer-by-layer assembly of microcapsules and their biomedical applications, *Chem. Soc. Rev.*, 2012, **41**, 6103–6124.
33 A. Vlachopoulos, G. Karlioti, E. Balla, V. Daniilidis, T. Kalamas, M. Stefanidou, *et al.*, Poly(Lactic Acid)-Based Microparticles for Drug Delivery Applications - An Overview of Recent Advances, *Pharmaceutics*, 2022, **14**, 359, DOI: 10.3390/pharmaceutics14020359.
34 S. Fredenberg, M. Wahlgren, M. Reslow and A. Axelsson, The mechanisms of drug release in poly(lactic-co-glycolic acid)-based drug delivery systems - A review, *Int. J. Pharm.*, 2011, **415**, 34–52.
35 E. H. Nafea, A. M. L. A. Poole-Warren and P. J. Martens, Immunoisolating semi-permeable membranes for cell encapsulation: Focus on hydrogels, *J. Controlled Release*, 2011, **154**, 110–122.
36 P. Trucillo, Drug Carriers: A Review on the Most Used Mathematical Models for Drug Release, *Processes.*, 2022, **10**, 1094, DOI: 10.3390/pr10061094.
37 Fortune Business Insights, Drug Delivery Systems Market, 2022–2029, 2023https://www.fortunebusinessinsights.com/drug-delivery-systems-market-103070.
38 J. F. Coelho, P. C. Ferreira, P. Alves, R. Cordeiro, A. C. Fonseca, J. R. Góis, *et al.*, Drug delivery systems - Advanced technologies potentially applicable in personalized treatments, *EPMA J.*, 2010, **1**, 164–209.
39 Y. Hu, S. Hu, S. Zhang, S. Dong, J. Hu, L. Kang, *et al.*, A double-layer hydrogel based on alginate-carboxymethyl cellulose and synthetic polymer as sustained drug delivery system, *Sci. Rep.*, 2021, **11**, 9142, DOI: 10.1038/s41598-021-88503-1.
40 Q. Li, X. Li and C. Zhao, Strategies to Obtain Encapsulation and Controlled Release of Small Hydrophilic Molecules, *Front. Bioeng. Biotechnol.*, 2020, **8**, 437, DOI: 10.3389/fbioe.2020.00437.
41 K. Moore, J. Amos, J. Davis, R. Gourdie and J. D. Potts, Characterization of polymeric microcapsules containing a low molecular weight peptide for controlled release, *Microsc. Microanal.*, 2013, **19**, 213–226.
42 A. C. Lima, P. Sher and J. F. Mano, Production methodologies of polymeric and hydrogel particles for drug delivery applications, *Expert Opin. Drug Deliv.*, 2012, **9**, 231–248.
43 M. D. Neto, M. B. Oliveira and J. F. Mano, Microparticles in Contact with Cells: From Carriers to Multifunctional Tissue Modulators, *Trends Biotechnol.*, 2019, **37**, 1011–1028.

This journal is © The Royal Society of Chemistry 2026

Open Access Article. Published on 06 May 2026. Downloaded on 6/20/2026 10:08:09 AM.
This article is licensed under a Creative Commons Attribution 3.0 Unported Licence.

44 S. Leick, A. Kemper and H. Rehage, Alginate/poly-l-lysine capsules: mechanical properties and drug release characteristics, *Soft Matter*, 2011, **7**, 6684.
45 P. A. M. Ferreira, J. P. Martins, J. Hirvonen and H. A. Santos, Spray-drying for the formulation of oral drug delivery systems, in *Nanotechnology for Oral Drug Delivery*, Elsevier, 2020, pp. 253–284.
46 I. Khan, K. Saeed, I. Zekker, B. Zhang, A. H. Hendi, A. Ahmad, *et al.*, Review on Methylene Blue: Its Properties, Uses, Toxicity and Photodegradation, *Water*, 2022, **14**, 242, DOI: 10.3390/w14020242.
47 Y. F. Li, C. Z. Huang and M. Li, A Resonance Light-Scattering Determination of Proteins with Fast Green FCF, *Anal. Sci.*, 2002, **18**, 177–181.
48 Y. Cui, Z. Tan, Y. Wang, S. Shi and X. Chen, One-step cross-linking preparation of tannic acid particles for the adsorption and separation of cationic dyes, *Chin. J. Chem. Eng.*, 2023, **57**, 309–318, DOI: 10.1016/j.cjche.2022.08.002.
49 N. Lakshani, H. S. Wijerathne, C. Sandaruwan, N. Kottegoda and V. Karunarathne, Release Kinetic Models and Release Mechanisms of Controlled-Release and Slow-Release Fertilizers, *ACS Agric. Sci. Technol.*, 2023, **3**, 939–956.